FORECASTING AUSTRALIAN DROUGHT USING SOUTHERN HEMISPHERE MODES OF SEA-SURFACE TEMPERATURE VARIABILITY

WARREN B. WHITE,[a,*] ALEXANDER GERSHUNOV,[a] JEFFREY L. ANNIS,[a] GREG MCKEON[b] and JOZEF SYKTUS[b]

[a] *Scripps Institution of Oceanography (SIO), University of California at San Diego, La Jolla, CA 92093-0230, USA*
[b] *Department of Natural Resources and Mines, 80 Meires Road, Indooroopilly, Queensland 4068, Australia*

ABSTRACT

Drought of 3 to 7 years' duration has devastated the flora, fauna, and regional economies in rangeland grazing districts over eastern and central Australia every 15 to 25 years throughout the 20th century, in some cases degrading the land beyond recovery. Recently, these drought and degradation episodes have been associated with a global interdecadal oscillation (IDO) of period 15 to 25 years. This IDO signal brought cooler sea-surface temperatures (SSTs) to the western extra-tropical South Pacific Ocean in association with reduced onshore transport of moisture over eastern/central Australia during the summer monsoon. Here, we utilize optimized canonical correlation analysis (CCA) to forecast principal components of summer precipitation (PCP) anomalies over Australia from the persistence of principal components that dominate spring SST anomalies across the Southern Hemisphere. These summer PCP forecasts are cross-validated with the CCA forecast model for each year independent of that year's variability. Resulting cross-validated forecasts are best over Queensland, correlating with those observed at >0.40 from 1890 through to 2001, significant at >99% confidence level. More importantly, 6 of 10 drought episodes (but only three of seven degradation episodes) observed in eastern/central Australia during the 20th century are forecast. Copyright © 2004 Royal Meteorological Society.

KEY WORDS: forecasting; Australian drought; canonical correlation analysis

1. INTRODUCTION

The history of grazing of sheep and cattle on Australia's rangelands over the 20th century is often characterized by boom and bust instigated by drought episodes of 3 to 7 years' duration that occur every 15 to 25 years from the late 1800s to the present (e.g. Donovan, 1995). Recently, McKeon *et al*. (2004) chronicled seven drought episodes that resulted in land degradation over six example rangeland grazing districts of eastern/central Australia (Table I). These degradation episodes occurred over western New South Wales from 1897 to 1902, over southeast Australia from 1927 to 1931, over western New South Wales from 1943 to 1945 and 1964 to 1966, over central Australia from 1960 to 1966, over southwest Queensland from 1964 to 1966, and over northeast Queensland from 1984 to 1988.

Below-normal precipitation (PCP) during the summer rainy season instigated degradation processes that included loss of desirable perennial vegetation, dust storms, drifting sands, loss of surface soil, reduced infiltration capacity, water-driven soil erosion, woody weed infestation, and rabbit plagues (McKeon *et al*., 1990). These processes devastated the flora and fauna over the land (Carter *et al*., 2000), and periodically throughout the 20th century brought ruin to regional economies, driving many stock enterprises into financial failure and worse. Most of the degradation episodes (Table I) led to major government inquiries and intervention. Sometimes these were followed by recovery periods in which favourable PCP resulted in

* Correspondence to: Warren B. White, Scripps Institution of Oceanography (SIO), University of California at San Diego, La Jolla, CA 92093-0230, USA; e-mail: wbwhite@ucsd.edu

luxurious plant and animal growth (Donovan, 1995). Other times, however, the productivity of land for grazing purposes did not return, leaving scalds and woody weeds in its wake (Beadle, 1948; Wilcox and Cunningham, 1993).

White *et al*. (2003) investigated the source of drought and degradation episodes during the summer rainy season over eastern/central Australia. They found summer PCP variability during the 20th century characterized by quasi-biennial, interannual, quasi-decadal, and interdecadal signals. Subsequently, they found these signals associated with corresponding signals in global sea-surface temperature (SST) and sea-level pressure (SLP) anomalies. These global climate signals are the familiar 2 to 3 year period quasi-biennial oscillation (QBO), the 3 to 7 year period El Niño−southern oscillation (ENSO), the 7 to 13 year period quasi-decadal oscillation (QDO), and the 15 to 25 year period interdecadal oscillation (IDO; White and Cayan, 1998; Allan, 2000; White and Tourre, 2003). White *et al*. (2003) found the Pacific extra-tropical cool phase of each of these global climate signals associated with higher SLP over northwest Australia and less onshore geostrophic transport of tropospheric moisture over eastern/central Australia during the summer monsoon. The latter resulted in summer dry conditions over land.

White *et al*. (2003) also found the interdecadal signal of 15 to 25 year period in summer PCP anomalies over eastern/central Australia dominating the higher frequency signals and fluctuating in phase with the global IDO signal. This accounted for the drought episodes of 3 to 7 years' duration that plagued Australia every 15 to 25 years throughout the 20th century. These drought episodes occurred during the decade straddling 1900, 1915, 1929, 1944, 1963, and 1982, coinciding with the Pacific extra-tropical cool phase of the global IDO signal (White and Tourre, 2003). The latter displayed the largest extra-tropical SST and SLP contrast across Australia from the south Indian Ocean to the South Pacific Ocean of the four QBO, ENSO, QDO, and IDO signals (White and Tourre, 2003). This may explain why drought is endemic to Australia.

The foregoing analysis of White *et al*. (2003) suggested that the optimized canonical correlation analysis (CCA) of Gershunov and Cayan (2003) might produce significant cross-validated forecasts of summer PCP anomalies over eastern/central Australia throughout the 20th century (i.e. 1890 through to 2001) from the persistence of Southern Hemisphere patterns of spring SST anomalies. Here, we test this hypothesis by constructing the 'best' CCA forecast model for summer PCP forecasts over the 112 year record. Each forecast is cross-validated by constructing the CCA forecast model anew each year so that it is independent of that year's variability. This is equivalent to testing the CCA forecast model on a time sequence of completely independent data (Box *et al*., 1994). The optimized CCA forecast methodology begins by finding Southern Hemisphere principal components of spring SST variability that best correlate with corresponding principal components of summer PCP variability over Australia. It uses canonical correlates to conduct the forecast of summer PCP patterns of variability from spring SST patterns of variability over the 112 year record. It optimizes the procedure by finding the number of principal components and the number of canonical correlates that achieve the highest forecast skill averaged over Australia. Reconstructing summer PCP anomalies over Australia from the 'best' forecast of summer PCP patterns of variability yields the forecast at each grid point. The optimized CCA forecast is found to work best over Queensland, where cross-validated forecasts of summer PCP anomalies correlate with those observed at >0.40 from 1890 through to 2001. This is significant at the 99% confidence level for the 112 year record. More importantly, over eastern/central Australia 6 of 10 drought episodes (but only three of seven degradation episodes) observed during the 20th century are forecast successfully.

2. DATA AND METHODS

2.1. Predictand and predictor data sets

The predictand is the seasonal PCP variability over Australia for summer (December, January, February) that has been interpolated from individual stations onto a 0.25° grid from 1890 through to 2001 (Jeffrey *et al*., 2001). Since computer resources were insufficient to conduct CCA forecast optimization on this relatively high-resolution grid, we interpolated the seasonal PCP data onto a 1° latitude−longitude grid and onto a 5° latitude−longitude grid. The 5° grid allows us to examine forecast skill on the national or state scale, and the 1° grid allows us to examine the forecast skill at the shire or grazing district scale. Examples of grazing districts

are identified by main town names, i.e. Charters Towers for Dalrymple shire and Quilpie for Murweh, Paroo and Quilpie shires. On the other hand, Alice Springs represents central Australia, and New South Wales and Queensland represent pastoral districts over all or portions of the respective states (see White *et al.* (2003)).

We focus on the five example grazing districts of White *et al.* (2003) because they experienced seven of the eight major degradation episodes occurring over all of Australia during the 20th century (Table I). The other degradation episode occurred in the Gascoyne grazing district in western Australia (not shown). This latter region has been excluded from this study because summer PCP variability is not a major component of its annual PCP variability.

The example grazing districts of Charters Towers, Quilpie, and Queensland are dominated by summer PCP variability. The grazing districts of Alice Springs and New South Wales have a significant winter/spring PCP variability component that also contributes to pasture growth. This is not included here. The contribution of winter/spring PCP variability to annual PCP variability is greater the further south the district is located. Nevertheless, the summer PCP variability is important even in southern districts because of the type of pasture plants that grow. They are typically perennial grasses, which produce stem and leaf under warm growing conditions. Stem tissues have a slower rate of decomposition and, hence, produce a low-quality feed and, more importantly, surface soil protection. Perennial grass tussocks are sites for improved PCP infiltration and the litter from perennial grasses also reduces overland flow. Thus, the lack of summer PCP in more southern regions of eastern Australia increases the risk of degradation processes, such as increased runoff and soil loss (McKeon *et al.*, 1990). Not surprisingly then, the degradation episodes in Table I are associated with drought in summer PCP variability.

The predictor is the seasonal SST variability over the globe and the Southern Hemisphere for spring (September, October, November) that has been interpolated from individual observations onto a 2° latitude–longitude grid at the Hadley Centre from 1890 through to 1998 (Folland and Powell, 1994; Parker *et al.*, 1994). To extend this SST record through to 2001, we combine it with spring SST anomalies from the National Centers for Environmental Prediction from 1950 through to 2001, also interpolated on a 2° latitude–longitude grid (Reynolds and Marsico, 1993; Kalnay *et al.*, 1996). We combine the SST variability from these two sources to construct a record of global and Southern Hemisphere spring SST variability from 1890 through to 2001. Because computer resources were insufficient to conduct the forecast optimization on the 2° latitude–longitude grid, we interpolated the SST data onto a 4° latitude by 8° longitude grid. We utilize two domains. One is more global in extent (i.e. 20 °N–50 °S, 30 °E–30 °E) and the other is confined to the south Indian and South Pacific Oceans surrounding Australia (i.e. 10–50 °S, 30 °E–160 °W).

We forecast summer PCP variability over Australia using other variables as the predictor as well, i.e. anomalous spring SLP, zonal surface wind (ZSW), meridional surface wind (MSW), and PCP over Australia. However, we found spring SST variability yielding better cross-validated forecasts than those of spring SLP and MSW variability, probably because the latter two were noisier. Spring SST variability also yields better forecasts than spring PCP variability over Australia, even though Simmonds and Hope (1997) found significant persistence in monthly PCP variability over Australia. On the other hand, we found spring ZSW variability yielding comparable forecasts, but for different parts of Australia (i.e. in southeast and western Australia). These forecasts will be reported in a separate study.

2.2. Multi-taper method–singular value decomposition methodology

To confirm that seasonal SST and Australian PCP anomalies display similar climate signals, we apply the multi-taper method (MTM)–singular value decomposition (SVD) methodology of Mann and Park (1999) to the global and Southern Hemisphere SST data sets from 1890 through to 2001, and to the Australian PCP data set for the same period. This produces a local fractional variance spectrum that yields the fraction of variance in a particular narrow frequency band associated with the dominant complex SVD mode over the 112 year record. The separation of the total variance into a discrete number of narrow-band signals is statistically significant, yielding spatially coherent global travelling waves and standing modes within the SST data set that apparently stamp their imprint on the Australian PCP data set. Here, we display the dominant spatial patterns of shared signals in SST and Australian PCP, together with amplitude time sequences of the corresponding narrow-band signals.

2.3. Optimized CCA forecast methodology

CCA was first used in diagnostic and predictive studies of climate variability by Barnett and Preisendorfer (1987). Applied to geophysical data, CCA is efficient at matching patterns in two fields of space−time data, making it ideal for statistical climate prediction when the predictor data set leads the predictand data set by some reasonable lead time. Since there are more observations in space (i.e. variables) than time steps (i.e. observations), both predictor and predictand fields are prefiltered using principal component analysis as a data reduction technique. Barnston and Smith (1996) applied CCA to diagnose and forecast global terrestrial PCP patterns from global SST variability. Our methodology differs from theirs by including a fully cross-validated optimization module that gives the approximately optimal model complexity (i.e. number of patterns (principal components) and the number of relationships (canonical correlates)) required to describe the coupled structure of the predictor−predictand fields efficiently (Gershunov and Cayan, 2003). In order to give realistic forecast skill estimates, leave-one-year-out cross-validation is used throughout in the optimization module, as well as in the skill estimation with the approximately optimal model (Box *et al.*, 1994). This means that, for every year of the 112 year record, the forecast model was re-estimated starting with principal component analysis on the remaining 111 years of data. Observed spring SST variability for year n was used to estimate (i.e. forecast) summer PCP variability via a model constructed from the remaining $n − 1$ years. This is a successful strategy because patterns of SST and Australian summer PCP variability have already been linked through the influence of SST variability on the summer monsoon that brings moisture onshore over eastern and central Australia from the western South Pacific Ocean. Note that no temporal filtering of either spring SST variability (i.e. the predictor) or summer PCP variability (i.e. the predictand) fields is used in the forecast portion of the study.

Once the cross-validated forecast is computed over Australia for each summer in the observation record, forecast skill is estimated simply as the correlation coefficient between the cross-validated forecast and the observed summer PCP variability at each location throughout the record. This yields maps of cross-validated forecast skill over Australia, and allows the time sequences of forecast and observed PCP variability at any location to be constructed over the 112 year record. Here, we focus on those regions in eastern/central Australia that experienced degradation episodes (Table I) during drought episodes. For the 112 year record, forecast skill is significant at the 99% (95%) level when it exceeds 0.28 (0.20) (Snedecor and Cochran, 1980). Details of the optimized CCA forecast methodology are given by Gershunov and Cayan (2003).

3. COVARYING SIGNALS IN AUSTRALIAN PCP AND SOUTHERN HEMISPHERE SST VARIABILITY

We begin by revealing the signals in global (20 °N to 50 °S) SST variability, Southern Hemisphere (10−50 °S, 30 °E−160 °W) SST variability, and Australian PCP variability over the 112 year record from 1890 through to 2001. We apply the MTM−SVD analysis of Mann and Park (1999) to these three data sets independently, computing the local fractional variance spectrum of each (Figure 1). These spectra display signals rising significantly above the background noise at the 95% confidence level. The three spectra together share a QBO signal near a 2.8 year period, ENSO signals near 4.4 and 5.8 year periods, a QDO signal near a 9.0 year period, an IDO signal ranging from a 15 to 30 year period, and a multidecadal signal for periods >30 years. The spectrum of the Australian PCP variability (Figure 1(a)) resembles those of Southern Hemisphere SST variability (Figure 1(b)) and global SST variability (Figure 1(c)). Since the latter is a subset of the former, this indicates that signals dominating Australian PCP variability are associated with signals dominating Southern Hemisphere SST variability.

The signals in the local fractional variance spectra (Figure 1) correspond to SVD modes, composed of spatial patterns (Figure 2) that are modulated by time sequences of amplitude (Figure 3). We display the amplitude time sequences for the QBO signal ranging from a 2.5 to 3.0 year period, the two ENSO signals ranging from a 4.0 to 5.0 year period and from a 5.0 to 7.5 year period, the QDO signal ranging from a 7.5 to 11.0 year period, the IDO signal ranging from a 15 to 30 year period, and the multidecadal signal for periods >30 years (Figure 3(a)−(f)). Forming these amplitude time sequences requires band-pass filtering
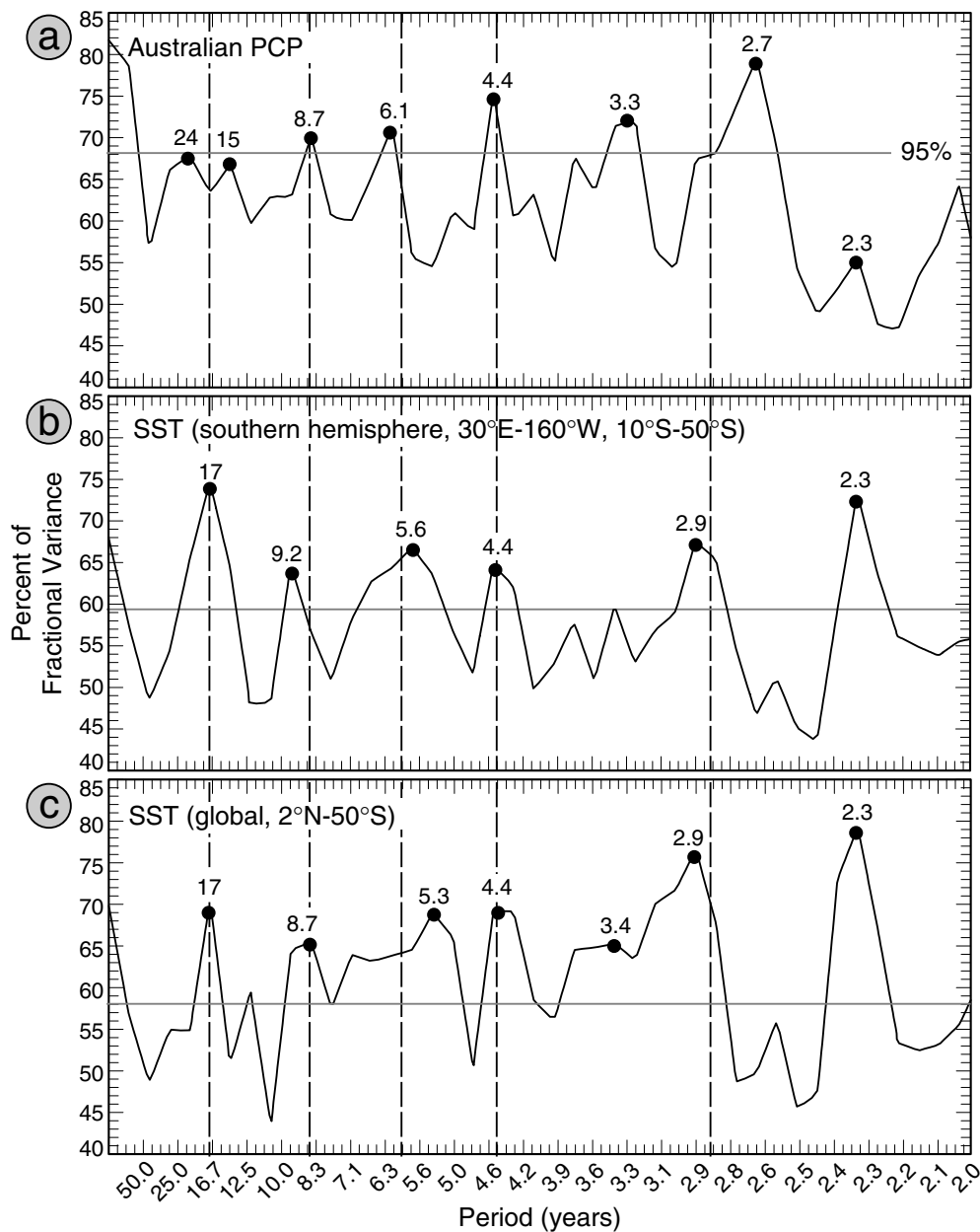
Figure 1. The MTM–SVD local fractional variance spectra of monthly anomalies of (a) Australian PCP, (b) SST over the Southern Hemisphere from 10°S to 50°S, 30°E to 160°W, and (c) SST over the globe from 20°N to 50°S, 30°E to 30°E. Horizontal lines represent the 95% confidence level. Vertical lines are used to align signals whose percentage variance rises above the 95% confidence level in each spectrum. The period is given in years along the abscissa and spectral magnitude along the ordinate is the percentage of variance explained by the dominant SVD mode in each frequency band (Mann and Park, 1999)

seasonal Australian PCP and Southern Hemisphere SST anomalies for the frequency bands encompassing each signal, and conducting the SVD analysis on the filtered anomalies, as performed by Allan (2000). Amplitude time sequences of SST and PCP SVD modes for each signal correlate with each other at >0.46 over the 112 year record, except for multidecadal variability. This is significant at the 95% confidence level, indicating that >21% of the seasonal PCP variability over eastern/central Australia is significantly associated

with seasonal SST anomalies over the surrounding ocean from 1890 through to 2001. The positive phase of each signal (Figure 3(a)–(e)) corresponds to a pattern of wet (dry) PCP weights over the eastern/central Australia (Figure 2, right) associated with a pattern of warm (cool) SST weights over the western extra-tropical South Pacific Ocean (Figure 2, left). The latter extended into the Southern Ocean south of Australia and into the south Indian Ocean with increasing period (Figure 2, left).

Comparing the amplitude time sequence of the interdecadal signal in seasonal PCP variability with those of the higher frequency signals finds its magnitude larger by nearly a factor of two, e.g. with the RMS for the interdecadal variability of 2.3 mm month^{-1} nearly twice that for the ENSO variability of 1.2 mm month^{-1} (Figure 3). Comparing the SST spatial pattern of the IDO signal with those of the other signals finds warm SST weights surrounding Australia on the north, east, and south sides more so than with those of the higher frequency signals (Figure 2, left). This is consistent with the spatial patterns associated with global QBO,
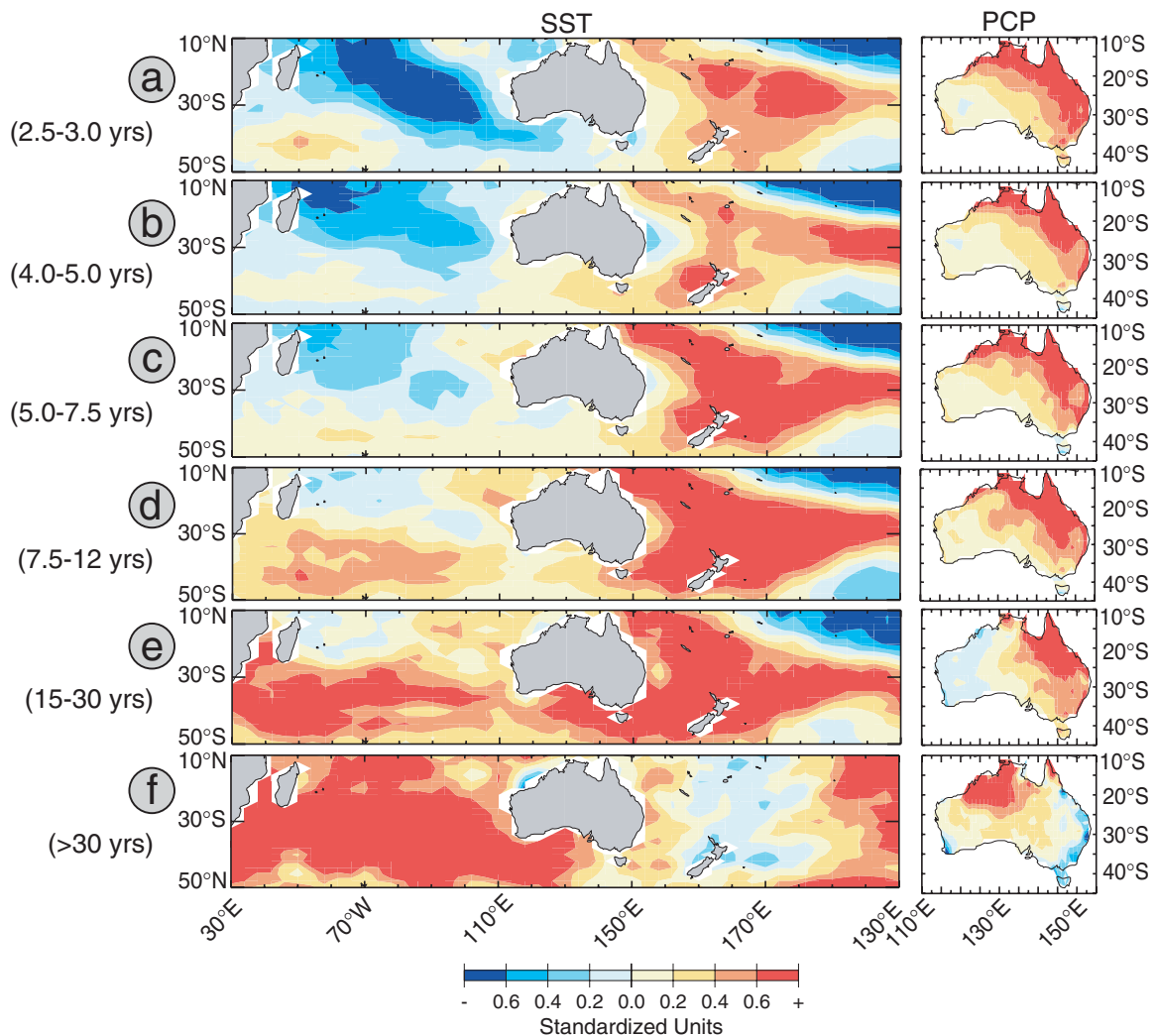

Figure 2. The spatial patterns of the dominant SVD modes for Australian PCP and Southern Hemisphere SST variability for (a) the QBO signal ranging in period from 2.5 to 3 years, (b) the ENSO signal ranging in period from 4.0 to 5.0 years, (c) the ENSO signal ranging in period from 5.0 to 7.5 years, (d) the QDO signal ranging in period from 7.5 to 12 years, (e) the IDO signal ranging in period from 15 to 30 years, and (f) the multidecadal signal for periods >30 years. The weights in each principal component pattern are normalized, with colour bar given at bottom, so that the magnitude of the variability is carried by the time sequence of amplitudes given in Figure 3
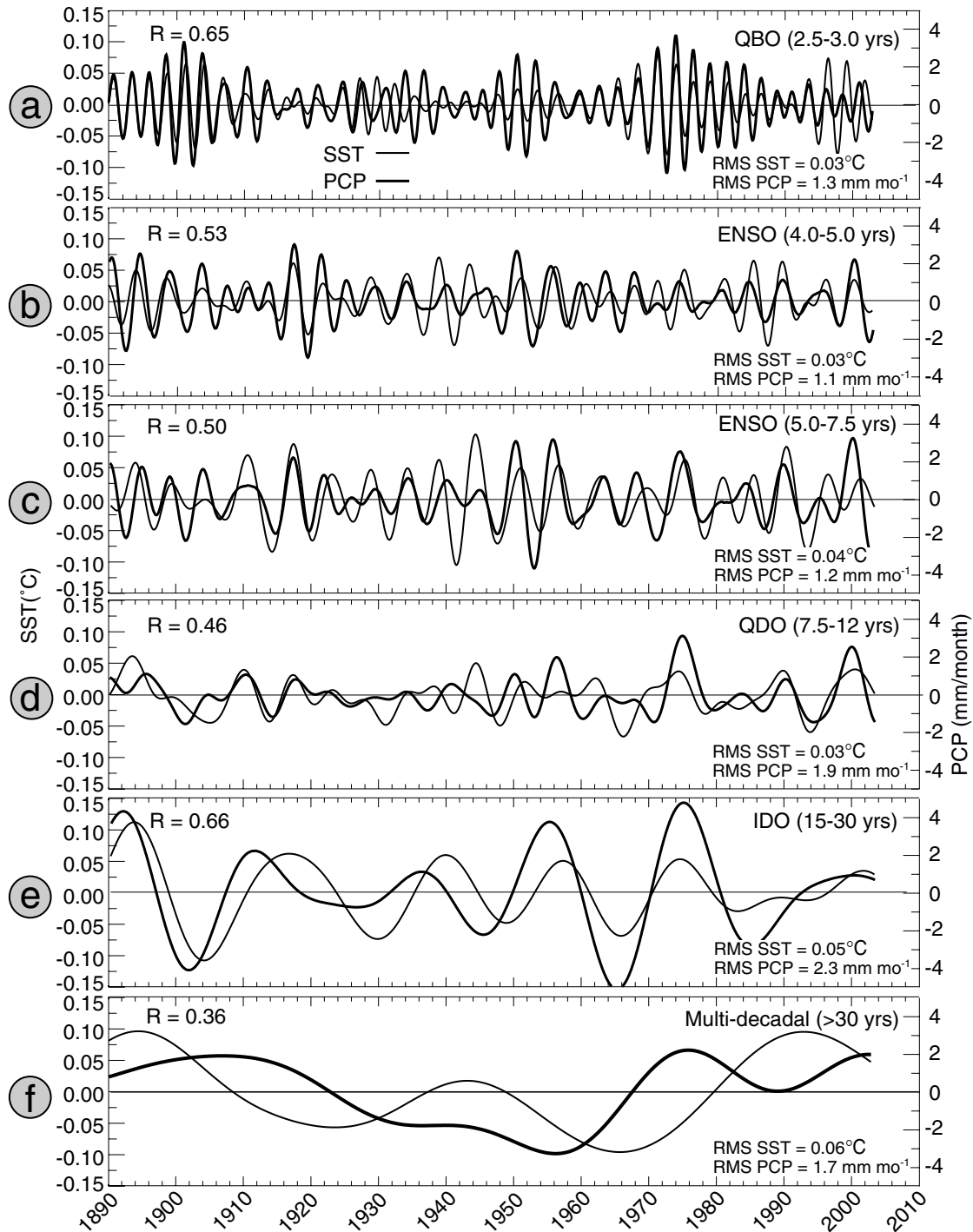
Figure 3. The time sequences of amplitude modulating the dominant SVD modes for Australian PCP and Southern Hemisphere SST variability for (a) the QBO signal ranging in period from 2.5 to 3 years, (b) the ENSO signal ranging in period from 4.0 to 5.0 years, (c) the ENSO signal ranging in period from 5.0 to 7.5 years, (d) the QDO signal ranging in period from 7.5 to 12 years, (e) the IDO signal ranging in period from 15 to 30 years, and (f) the multidecadal signal for periods >30 years. The correlation between the two time sequences is given in the upper left corner of each panel. The root-mean-square (RMS) of the variability is given in the lower right corner of each panel. The magnitude of each mode ranges over ±5.0 mm month^{-1} and ±0.15 °C

ENSO, QDO, and IDO signals (Allan, 2000; White and Tourre, 2003). On the other hand, the four signals in PCP variability display PCP spatial patterns that differ very little from one another over eastern/central Australia (Figure 2, right). Furthermore, the cross-correlation between amplitude time sequences of the interdecadal signals in both SST and PCP variability is 0.66, significant at the 97% confidence level for ∼12 effective degrees of freedom (Snedecor and Cochran, 1980) (Figure 3(e)). This indicates that ∼44% of the interdecadal PCP variability, which explains most of the drought cycle over eastern/central Australia (White *et al.*, 2003), is associated with the IDO pattern of Southern Hemisphere SST variability. Here, we find cool SST variability over the South Pacific Ocean and the Southern Ocean south of Australia accompanying drought over eastern/central Australia. This association is consistent with that observed by White *et al.* (2003), who found a similar pattern of SST variability in the IDO signal accompanied by high SLP variability over northwest Australia, reducing the onshore geostrophic transport of tropospheric moisture over eastern/central Australia during the summer monsoon.

4. SUMMER PCP VARIABILITY OVER EASTERN/CENTRAL AUSTRALIA

We display the summer PCP variability from the 5° latitude−longitude seasonal PCP data set located near the centre of the five domains (Figure 4), where degradation episodes occurred during the 20th Century (Table I). This includes the 5° latitude−longitude grid point closest to Canberra, Australia's capital. These summer PCP indices for Charters Towers, Queensland, Quilpie, New South Wales, Canberra, and Alice Springs each display drought episodes, defined by summer PCP anomaly being ≤0 for 3 to 7 years' duration. According to this definition, drought was widespread from 1897 to 1902, restricted to New South Wales and Canberra from 1912 to 1916 and 1929 to 1933, restricted to Alice Springs from 1925 to 1935, restricted to Queensland, Quilpie, and Charters Towers for most of 1930 to 1940, restricted to Canberra and New South Wales from 1942 to 1945, widespread from 1964 to 1967, restricted to Alice Springs from 1955 to 1965, restricted to Charters Towers, Queensland, and Quilpie from 1983 to 1990, restricted to New South Wales and Canberra over most of 1977 to 1985, and restricted to Charters Towers from 1993 to 1997. This sums to 10 drought episodes over the 20th century. These drought episodes form the larger set from which the degradation episodes are drawn (Table I), since degradation episodes respond to other factors, either geographical or sociological, that exacerbate the local drought phenomenon. We have highlighted drought episodes (Figure 4), finding them occurring every 15 to 25 years, centred near 1900, 1915, 1931, 1935, 1944, 1960 to 1965, 1983 to 1987, consistent with the degradation episodes in Table I. The drought episodes coincide roughly with the Pacific extra-tropical cool phase of the IDO signal in 1900, 1915, 1929, 1944, 1963, and 1982 (White and Tourre, 2003).

5. THE OPTIMIZED CCA FORECAST OF SUMMER PCP VARIABILITY OVER AUSTRALIA

We can now construct the CCA forecast model that optimizes the cross-validated skill of summer PCP variability over Australia. This CCA model uses antecedent spring SST patterns of variability over the Southern Hemisphere (10−50 °S, 30 °E−160 °W) as predictors of the summer PCP patterns of variability. It takes advantage of the persistence of SST patterns of variability from spring to summer that influence the monsoon circulation bringing summer rainfall to Australia. The optimized CCA forecast methodology is very efficient at finding covarying patterns of variability in the predictor and predictand, as shown by Gershunov and Cayan (2003).

   The optimum CCA model finds two principal components and two canonical correlates that yield the best cross-validated forecast skill averaged over Australia. The reason for this is clear from inspection of the amplitude time sequences that modulate the best-fit patterns of Australia summer PCP variability and Southern Hemisphere spring SST variability (Figure 5(a) and (b)). The amplitude time sequence of an SST principal component for spring (i.e. the predictor) that correlates best (i.e. $R = 0.42$) with that of an Australian PCP principal component for summer (i.e. the predictand) is dominated by an upward trend and by interdecadal variability (Figure 5(a)). The amplitude time sequence of an SST principal component for spring (i.e., the
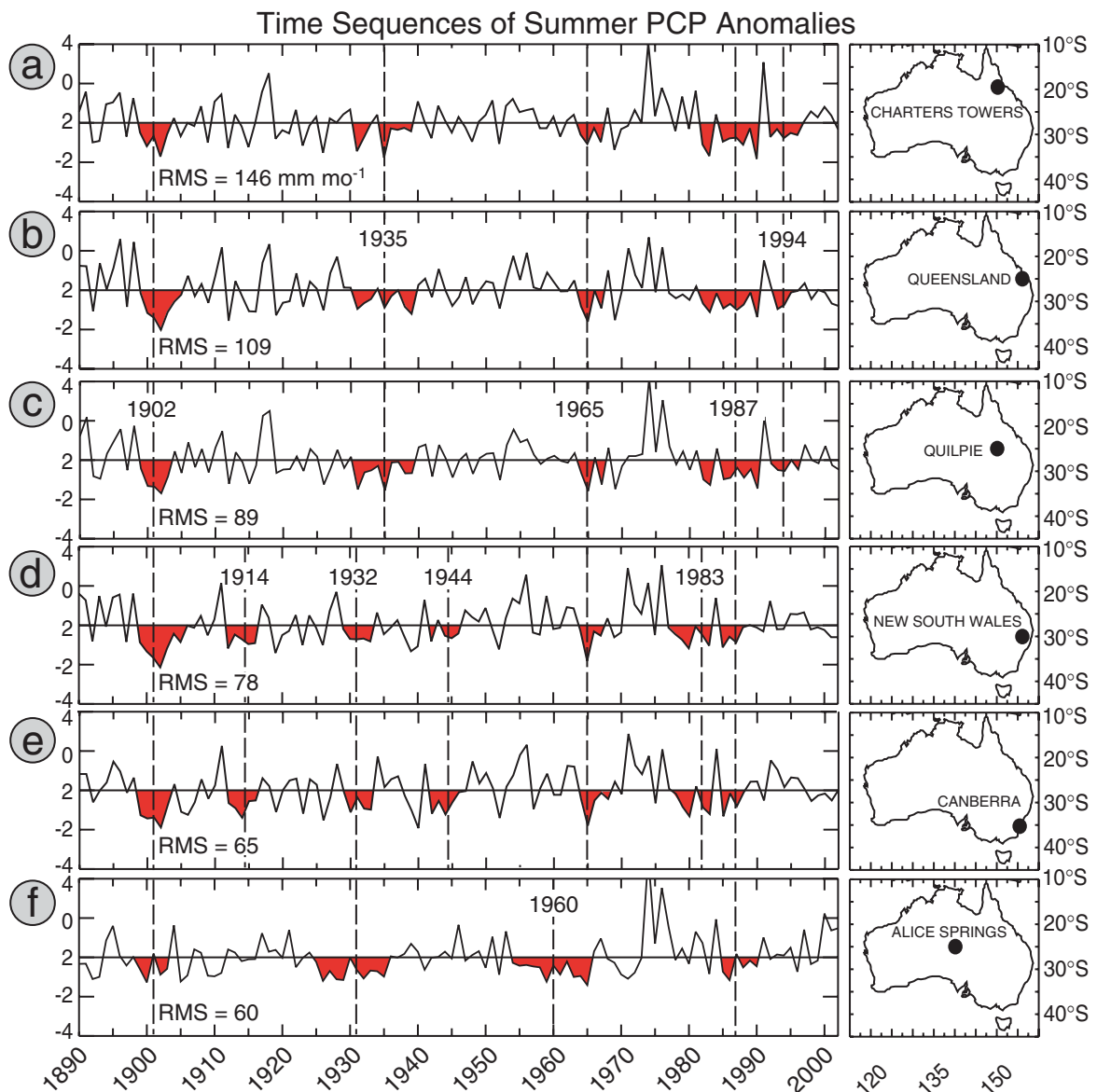
Figure 4. Time sequences of summer PCP anomalies for (a) Charters Towers, (b) Queensland, (c) Quilpie, (d) New South Wales, (e) Canberra, and (f) Alice Springs, the geographical locations of which are displayed at right. The summer season includes December, January, and February. Time sequences extend over 112 years from 1890 through to 2001. Time sequences are based on summer PCP anomalies interpolated onto the 5° latitude–longitude grid. Drought episodes in each time sequence are shaded. Each time sequence is normalized, with magnitude ranging over plus/minus four standard deviations, with the RMS of variability (mm month^{-1}) given in the lower left corner of each panel. Vertical dashed lines indicate years and locations of drought episodes occurring over the 112 year record. This figure is available in colour online at http://www.interscience.wiley.com/ijoc

predictor) that correlates second best (i.e. $R = 0.37$) with that of an Australian PCP principal component for summer (i.e. the predictand) is dominated by interdecadal and quasi-decadal variability (Figure 5(b)). Note that in the latter time sequence the summer PCP weights over eastern/central Australia are negative near 1900, 1915, 1942, 1965, and 1985, as occurs in the time sequence of drought episodes (Figure 4).

The spatial patterns of Southern Hemisphere SST and Australian PCP variability for the dominant pair of principal components (Figure 5(c) and (e)) has western and central Australian PCP higher than normal

Table I. Regional degradation episodes for six example rangeland grazing districts over Australia's rangelands (McKeon and Hall, 2002)

Episode	Degradation episodes	Period
1	1890–1900 in western New South Wales involving soil erosion, woody weed increase, rabbit plagues, substantial financial losses, resulting in Royal Commission of 1901 (Anon., 1901; Noble, 1997)	1897–1902
2	1920–30s in southeast Australia involving substantial loss of perennial vegetation and soil erosion (Ratcliffe, 1937), resulting in government legislation for regulation of carrying capacity (Donovan, 1995)	1927–31
3	1940s in western New South Wales involving substantial dust storms (Condon, 2002) and animal losses graphically portrayed in Russell Drysdale's paintings and Newman's newspaper reports and supporting the need for government action (Beadle, 1948)	1943–45
4	1960s in western New South Wales involving large increases in woody weeds, resulting in reduced carrying capacity and income (Anon., 1969; Hodgkinson *et al.*, 1984)	1964–66
5	1960s in central Australia involving wind and water erosion, resulting in extensive surveys and reassessment of carrying capacity (Condon *et al.*, 1969a–d; Purvis, 1986)	1960–66
6	1960s in southwest Queensland involving soil erosion and woody weed invasion, resulting in the government-sponsored South-West Strategy supporting review of recommended carrying capacities and property amalgamation (Warrego Graziers Association, 1988; Johnston *et al.*, 1996)	1964–66
7	1980s in northeast Queensland involving soil erosion and loss of desirable perennial grasses, resulting in extensive government-sponsored surveys (Rogers *et al.*, 1997) and dramatic grazier response (Landsberg *et al.*, 1998)	1984–88

when the warm SST variability surrounding Australia is largest in the Southern Ocean south of Australia. The corresponding spatial patterns for the sub-dominant pair of principal components (Figure 5(d) and (f)) have eastern (western) Australia PCP higher (lower) than normal when the warm (cool) SST variability occurs in the western extra-tropical South Pacific Ocean (eastern extra-tropical south Indian Ocean).

When this 'best' CCA forecast model (i.e. including the two foregoing principal component pairs) is cross-validated, it yields forecast skill >0.2 over most of Australia (Figure 5(g) and (h)), larger over eastern and central Australia (i.e. >0.3) where the degradation episodes occurred during the summer rainy season (Table I). The histogram of forecast skill on the 1° latitude–longitude grid over Australia is significantly different from that obtained when the patterns of Southern Hemisphere SST anomalies are asked to produce a 'best' forecast of noise over Australia (Figure 5(g)). The latter yields an average forecast skill of <0.01 over Australia, confirming the absence of artificial forecast skill in the optimized CCA forecast methodology. When Australian PCP data are interpolated onto a 5° latitude–longitude grid, the forecast skill over eastern Australia becomes larger still (i.e. >0.4). This increased forecast skill arises from two sources: (1) the resulting PCP variability displays the same spatial scale as that of SST variability and of summer monsoon processes that link the two variables (White *et al.*, 2003); (2) inherent spatial averaging acts to suppress random noise in the summer PCP variability. Thus, forecast skill for Australian summer PCP at the national scale will always be higher than on the shire (grazing district) scale.

6. CROSS-VALIDATED FORECASTS OF SUMMER PCP VARIABILITY OVER EASTERN/CENTRAL AUSTRALIA

Now we overlay the cross-validated forecasts of summer PCP variability on the time sequences of those observed near Charters Towers, Quilpie, Queensland, New South Wales, Canberra, and Alice Springs (Figure 6). Here, we utilize the forecasts for summer Australian PCP variability on the 5° latitude–longitude grid, which are better than those on the 1° latitude–longitude grid (Table II). The forecast skill over these five locations ranges from 0.30 near Canberra to 0.41 near Charters Towers, and in general this is better over
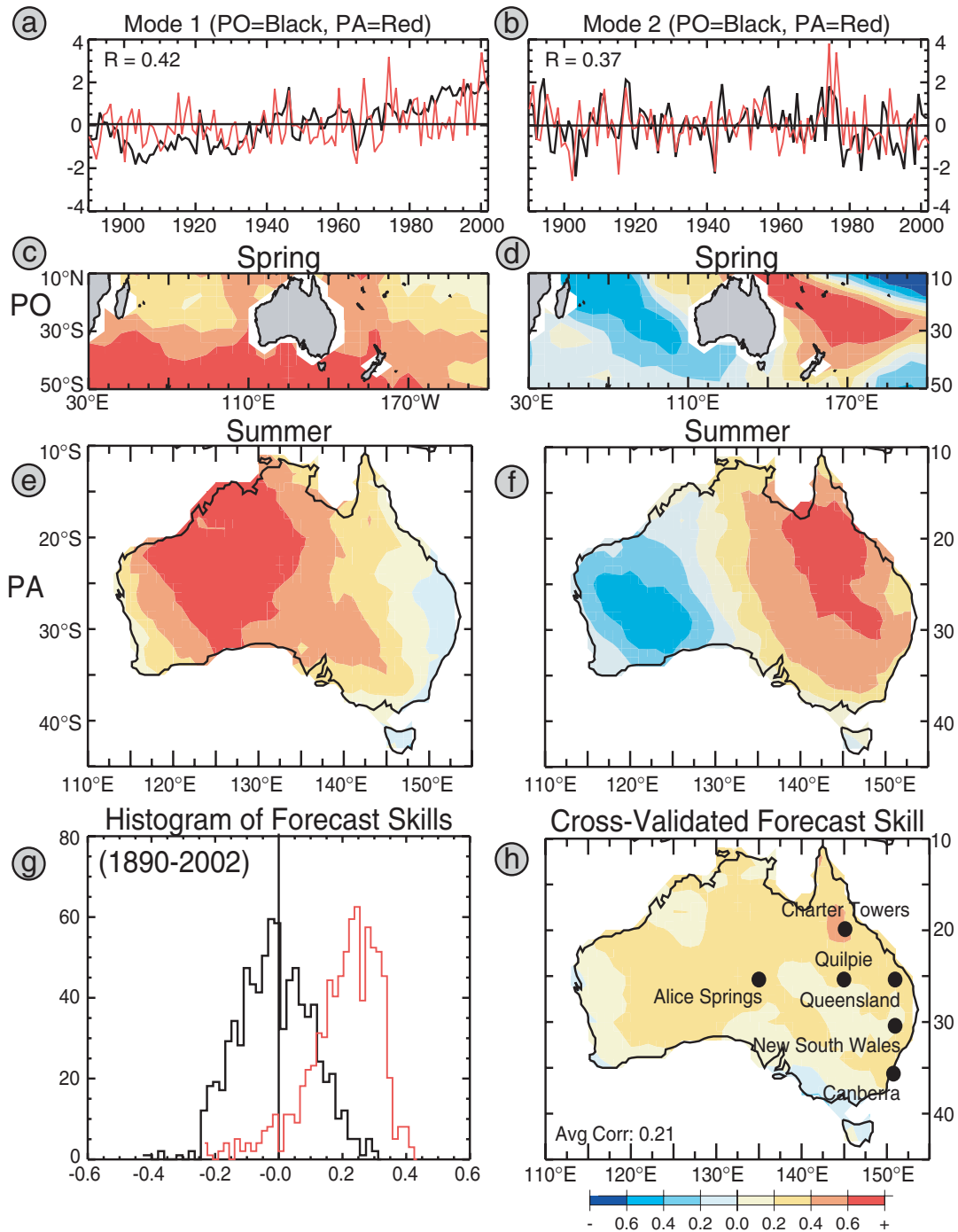
Figure 5. The cross-validated forecast of summer Australian PCP variability from spring SST variability over the Southern Hemisphere from 20 °S to 50 °S, 30 °E to 160 °W from an optimized CCA forecast model that seeks maximum cross-validated forecast skill averaged over Australia. (a and b) Amplitude time sequences of principal components of the spring SST predictor and the summer PCP predictand for the two modes that 'best' forecast the observed summer PCP variance. The magnitude ranges over plus/minus four standard deviations. (c–f) The normalized spatial patterns of the principal components of the predictor and predictand in (a) and (b), with the colour bar at the bottom showing standard deviation units in increments of 0.2. (g) Histograms of cross-validated forecast skill of observed summer PCP (noise) over Australia given by the red (black) curve. (h) Distribution of cross-validated forecast skill over Australia, with the colour bar below showing forecast skill in increments of 0.2

Table II. Average forecast skill for Australia summer PCP variability (1890–2002)

Grid resolution	Global		Southern Hemisphere	
	$1° \times 1°$	$5° \times 5°$	$1° \times 1°$	$5° \times 5°$
Charter Towers	0.42	0.43	0.42	0.41
Queensland	0.38	0.43	0.35	0.40
Quilpie	0.22	0.39	0.23	0.36
New South Wales	0.24	0.40	0.19	0.35
Canberra	0.32	0.35	0.31	0.30
Alice Springs	0.23	0.32	0.23	0.32

northeast Australia than over southeast Australia (Figure 5(h)). As important, we find the optimized CCA model producing realistic forecasts for most of the drought episodes that occurred over the 20th century (Figure 4), and for three of the seven degradation episodes (Table I).

The widespread drought episode of 1897 to 1902 (Figure 6(a)–(f)) that instigated the degradation episode in western New South Wales from 1897 to 1902 (1, Table I) is forecast successfully, with the forecast summer PCP in New South Wales normal or below normal from 1986 to 1906 (Figure 6(d)), which was longer and deeper than for the other locations over eastern and central Australia. The drought episode that afflicted New South Wales and Canberra from 1912 to 1916 (Figure 6(d) and (e)), and did not result in a degradation episode (Table I), is forecast successfully, with forecast summer PCP in New South Wales and Canberra normal and below normal from 1912 to 1916. The drought episodes that afflicted New South Wales and Canberra from 1929 to 1931 and that afflicted Alice Springs from 1925 to 1935 (Figure 6(d)–(f)), and resulted in a degradation episode over southeast Australia from 1927 to 1931 (2, Table I), are forecast successfully, with forecast summer PCP at New South Wales and Canberra below normal from 1929 to 1933 and below normal at Alice Springs from 1923 to 1935. The drought episode that afflicted Charters Towers, Queensland, and Quilpie from 1931 to 1939 (Figure 6(a)–(c)), and did not result in a degradation episode (Table I), is forecast successfully, with normal or below-normal PCP from 1930 to 1937. Thus, the drought and degradation episodes from 1890 to 1940 are forecast successfully with the optimized CCA model.

The drought episode that afflicted Canberra and New South Wales from 1942 to 1945 (Figure 6(d) and (e)), and resulted in a degradation episode over western New South Wales from 1943 to 1945 (3, Table I), is not forecast successfully, with forecast summer PCP in New South Wales and Canberra experiencing a sharp downturn in 1942 at the beginning of the drought but followed by a sharp upswing in 1943 and 1944 when the drought began to take hold. The widespread drought episode from 1964 to 1967 (Figure 6(a)–(e)), resulting in a degradation episode over western New South Wales and Queensland from 1964 to 1966 (4 and 6, Table I), is not forecast successfully, with forecast summer PCP showing a sharp upswing in 1965 when observed PCP showed a sharp downswing. The drought episode that affected Alice Springs from 1955 to 1965 (Figure 6(f)), and resulted in a degradation episode over central Australia from 1960 to 1966 (5, Table I), is not forecast successfully, with forecast summer rainfall showing above-normal PCP from 1956 to 1963 when the observed PCP was below normal. Thus, drought and degradation episodes over the middle part of the 20th century from 1940 to 1965 are not forecast successfully.

The widespread drought episode from 1983 to 1989 (Figure 6(a)–(f)) that resulted in a degradation episode over Queensland from 1984 to 1988 (7, Table I) is forecast successfully, with forecast summer PCP over Queensland normal or below normal from 1978 to 1988 (Figure 6(b)). The drought episode that afflicted New South Wales and Canberra over most of 1977 to 1987 (Figure 6(d) and (e)), and did not result in a degradation episode (Table I), is forecast successfully, with normal or below-normal rainfall from 1976 to 1987. The drought episode that afflicted Charters Towers, Queensland, and Quilpie from 1993 to 1996 (Figure 6(a)–(c)), and did not result in a degradation episode (Table I), is forecast successfully, with normal or below-normal rainfall from 1991 to 1996 (Figure 6(a)–(c)). Thus, drought and degradation episodes from 1965 to 2000 are forecast successfully.
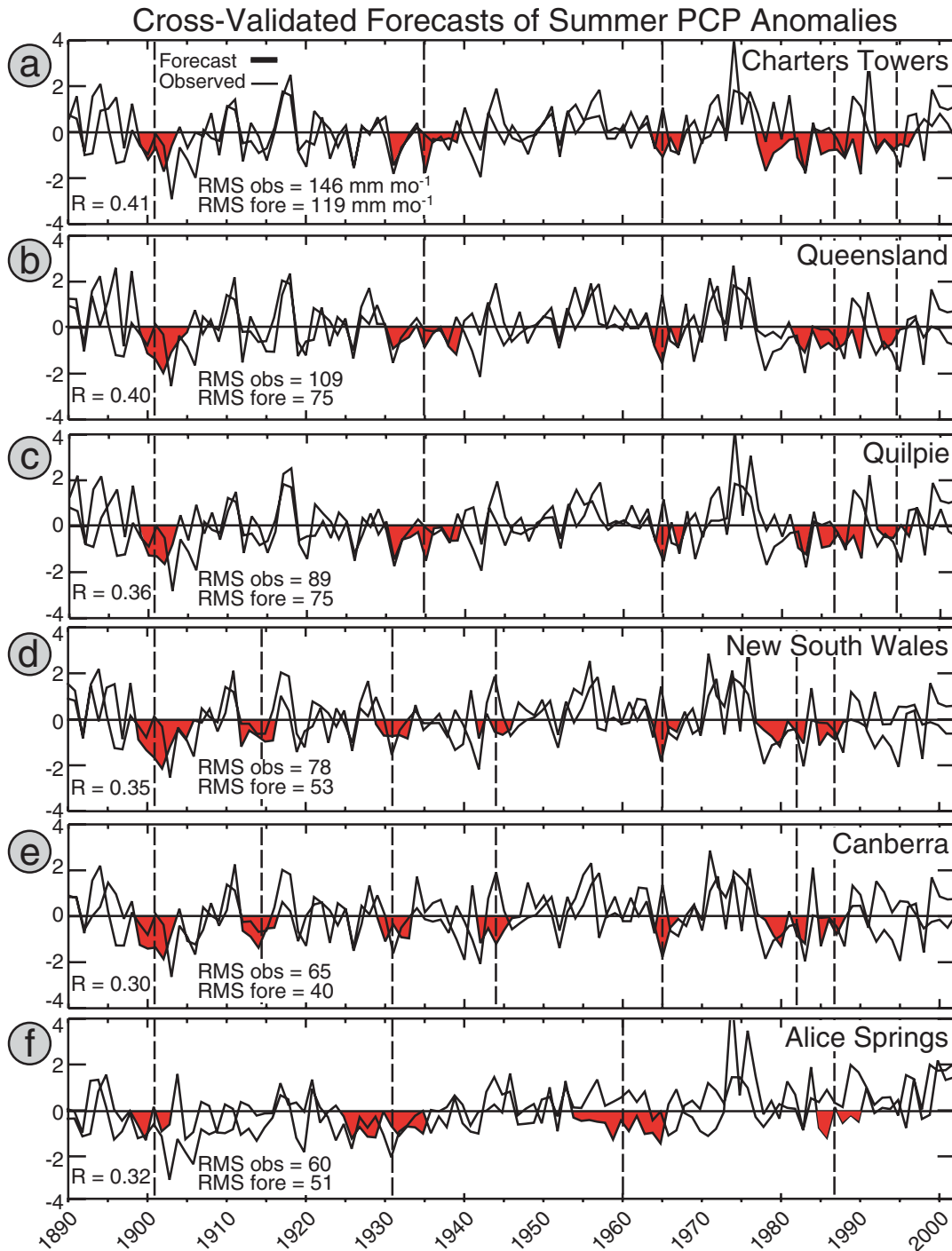
Figure 6. Time sequences of the observed (thin line) and cross-validated forecasts (thick line) for summer PCP anomalies for (a) Charters Towers, (b) Queensland, (c) Quilpie, (d) New South Wales, (e) Canberra, and (f) Alice Springs, the geographical locations of which are displayed in Figure 4. The summer season includes December, January, and February. Time sequences extend over 112 years from 1890 through to 2001. Observed and forecast time sequences are based on summer PCP anomalies interpolated onto the 5° latitude–longitude grid. Drought episodes are shaded, as in Figure 4. Each time sequence is normalized, with magnitude ranging over plus/minus standard deviations and with the RMS of variability (mm month^{-1}) given in the lower left corner of each panel. Vertical dashed lines indicate years and locations of drought episodes occurring over the 112 year record, consistent with Figure 4. This figure is available in colour online at http://www.interscience.wiley.com/ijoc

Thus, the three drought and two degradation episodes from 1890 to 1940 are forecast successfully with the optimized CCA model, but the four droughts and four degradation episodes over the middle part of the 20th century, from 1940 to 1965, are not. On the other hand, the three drought and one degradation episode from 1970 to 2000 are forecast successfully. So, 6 of 10 drought episodes and three of seven degradation episodes observed over eastern/central Australia during the 20th century are forecast successfully.

7. DISCUSSION AND CONCLUSIONS

We find the summer PCP variability over eastern/central Australia to be influenced significantly by the superposition of QDO, IDO, and multidecadal signals observed in global climate variability (Allan, 2000; White and Tourre, 2003). Previously, investigations have focused on the impact of the interannual ENSO signal on Australian PCP variability (e.g. Stone *et al*., 1994; Cai *et al*., 2001) and its interdecadal modulation (Power *et al*., 1999). Although the latter has a significant influence on the year-to-year changes in summer rainfall, it is the QDO, IDO, and multidecadal signals that influence the occurrence of drought episodes that have plagued Australian PCP variability during the 20th century (White *et al*., 2003). These latter signals cannot be found in spectra of the Niño-3 or Niño-3.4 SST indices typically used to characterize the interannual ENSO signal (White and Tourre, 2003), indicating the futility of utilizing El Niño indices to forecast drought conditions over Australia.

Although the global SST patterns of QDO and IDO signals bear some resemblance to that of the ENSO signal, they display maximum SST variability in the central and western tropical Pacific Ocean, and display greater SST variability over the extra-tropical oceans surrounding Australia (Allan, 2000; Tourre *et al*., 2001; White and Tourre, 2003). White *et al*. (2003) demonstrated that the anomalous paths of tropospheric moisture flux over eastern/central Australia during the summer monsoon were associated with QDO and IDO signals in the southeast trade winds that carry moisture over Australia from the tropical and subtropical South Pacific Ocean. In the present study, we applied the MTM−SVD analysis of Mann and Park (1999) to Australian summer PCP variability and global and Southern Hemisphere SST variability, finding the QBO, ENSO, QDO, and IDO signals in both records fluctuating together. However, the time sequences of each signal in Australian summer PCP variability finds the magnitude of the IDO signal dominating that of the higher frequency signals, explaining again why summer PCP variability in eastern/central Australia is dominated by drought occurring every 15 to 25 years.

The objective of the present study is to determine whether the persistence of spring SST patterns of variability over the Southern Hemisphere oceans surrounding Australia can be used to forecast summer PCP variability over eastern/central Australia in cross-validated fashion. Indeed, we find this to be the case, utilizing the optimized CCA forecast scheme of Gershunov and Cayan (2003). The latter includes a fully cross-validated optimization module that gives the optimal model complexity (i.e. number of patterns (principal components) and the number of relationships (canonical correlates)) required to describe the coupled structure of the predictor−predictand fields efficiently. We find the dominant principal components of spring SST variability over the Southern Hemisphere (i.e. 10−50 °S, 30 °E−160 °W) yielding similar cross-validated forecast skill of Australian summer PCP variability as the global SST variability (20 °N−50 °S, 30 °E−30 °E) (Table II). This is consistent with the finding by White *et al*. (2003) that extra-tropical Southern Hemisphere SST patterns influence the intensity of the summer monsoon over eastern and central Australia. This is a different mechanism than the atmospheric bridge hypothesized to teleconnect ENSO influence from the equatorial Pacific Ocean (Cai *et al*., 2001). We also find the principal components of SST variability during the previous spring season yielding a better forecast of Australian summer PCP variability than extended principal components of SST variability over the previous two, three, four, or five seasons. This is because the pertinent principal components are dominated by QDO, IDO and multidecadal signals, in which case the slow eastward phase propagation of covarying SST and SLP anomalies associated with these signals (White and Tourre, 2003) does not improve the forecast from spring to summer.

Furthermore, we find the optimized CCA forecast model containing only two pairs of principal components out of a possible 10 pairs. The simplicity indicated by this low-order model system arises for two reasons. First,

it is consistent with the dominance of the QDO and IDO signals in summer PCP variability over eastern/central Australia (White *et al.*, 2003), which has drought episodes of 3 to 7 years' duration coinciding with cool SST anomalies in the tropical and extra-tropical oceans surrounding Australia. Second, it is consistent with the underlying summer monsoon circulation, whose intensity depends largely on the strength and location of the southeast trade winds accompanying the evolution of QDO and IDO signals in covarying SST and SLP variability across the western South Pacific Ocean (White *et al.*, 2003). The source of noise in the summer monsoon system, which may inhibit higher forecast skill from consideration of SST variability alone, derives from stochastic elements such as the 40- to 50-day waves transiting the tropical ocean (Madden and Julian, 1971). Even so, as a rule of thumb, when SST anomalies are warm (cool) over most of the western South Pacific Ocean and Southern Ocean surrounding Australia during spring, one must consider the possibility for greater (lesser) PCP over most of eastern/central Australia during the following summer.

We find the forecast skill higher when principal components of spring SST variability were used to forecast Australian summer PCP variability on a 5° latitude–longitude grid (national scale) over Australia than on the original 1° latitude–longitude grid (shire or grazing district scale) (Table II). This is because the coarse grid resolution suppresses sub-grid noise. Thus, cross-validated forecasts of summer rainfall over Queensland (New South Wales) correlate with those observed at 0.40 (0.35) on the national-scale resolution from 1890 through to 2001, whilst correlating with those observed at 0.35 (0.19) on the shire-scale resolution, with correlations exceeding 0.24 (0.19) significant at the 99% (95%) confidence level. Furthermore, droughts that occurred over all or different portions of eastern/central Australia during the periods 1897–1902, 1912–16, 1929–33, 1932–39, 1942–45, 1960–66, 1984–88, and 1993–97 are forecast or not forecast equally on both grid scales. The CCA model forecasts six out of the 10 drought episodes observed over eastern/central Australia from 1890 through to 2001, but only three of the seven degradation episodes. The CCA model was unable to forecast drought and degradation episodes occurring from 1940 to 1965, when most of the degradation episodes occurred. This epoch coincides with below-normal PCP variability in the multidecadal signal that was not matched by below-normal SST variability in the multidecadal signal (Figure 3).

What are the prospects for improving these forecast skills? They are excellent. First, we found the QDO, IDO, and multidecadal signals in spring ZSW variability over the Southern Hemisphere yielding comparable forecast skills for Australian summer PCP variability, but for different parts of Australia (i.e. western/central Australia). Thus, a multivariate forecast scheme including both SST and ZSW patterns can be expected to improve the cross-validated forecast skill averaged across Australia. Second, we can choose the optimum CCA model that does not yield the best forecast averaged over all of Australia, but for different regions of Australia. This can yield a different combination of principal components and canonical correlates that produce the best forecast of summer PCP variability in the region chosen. Furthermore, upon visually inspecting the degree of correlation between the forecast and observed summer rainfall in Figure 6, we find this varying on multidecadal period scales (e.g. poor from 1940 to 1965). This indicates that conditional cross-validated forecasts of the kind conducted by Gershunov and Barnett (1998; Gershunov *et al.*, 1999) can achieve significant improvement in forecast skill.

REFERENCES

Allan RJ. 2000. ENSO and climatic variability in the last 150 years. In *El Niño and the Southern Oscillation: Multiscale Variability, Global and Regional Impacts*, Diaz HF, Markgraf V (eds). Cambridge University Press: UK; 3–55.
Anon. 1901. *Royal Commission to Inquire into the Conditions of the Tenants, Western Division of New South Wales*. Government Printer: Sydney.

Anon. 1969. *Report of the Interdepartmental Committee on Scrub and Timber Re-growth in the Cobar–Byrock District and Other Areas of the Western Division of New South Wales*. Government Printer: Sydney.

Barnett TP, Preisendorfer R. 1987. Origins and levels of monthly and seasonal forecast skill for United States surface air temperatures determined by canonical correlation analysis. *Monthly Weather Review* **115**: 1825–1850.

Barnston AG, Smith TM. 1996. Specification and prediction of global surface temperature and precipitation from global SST using CCA. *Journal of Climate* **9**: 2660–2697.

Beadle NCW. 1948. *The Vegetation and Pastures of Western New South Wales with Special Reference to Soil Erosion*. Government Printer: Sydney.

Box GEP, Jenkins GM, Reinsel GC. 1994. *Time Series Analysis: Forecasting and Control*, 3rd edition. Prentice Hall: Englewood Cliffs, NJ.

Cai W, Whetton PH, Pittock AB. 2001. Fluctuations of the relationship between ENSO and the northeast Australia rainfall. *Climate Dynamics* **17**: 421–432.

Carter JO, Hall WB, Brook KD, McKeon GM, Day KA, Paul CJ. 2000. Aussie GRASS: Australian grassland and rangeland assessment by spatial simulation. In *Applications of Seasonal Climate Forecasting in Agricultural and Natural Ecosystems — the Australian Experience*, Hammer G, Nicholls N, Mitchell C (eds). Kluwer Academic Press: Netherlands.

Condon RW. 2002. Out of the west, historical perspectives on the Western Division. The Rangelands Management Action Program (RMAP), Wentworth, NSW.

Condon RW, Neuman JC, Cunningham GM. 1969a. Soil erosion and pasture degeneration in central Australia. Part I — soil erosion and degradation of pastures and topfeeds. *Journal of the Soil Conservation Service of New South Wales* **25**: 47–92.

Condon RW, Neuman JC, Cunningham GM. 1969b. Soil erosion and pasture degeneration in central Australia. Part II — prevention and control of soil erosion and pasture degradation. *Journal of the Soil Conservation Service of New South Wales* **25**: 161–182.

Condon RW, Neuman JC, Cunningham GM. 1969c. Soil erosion and pasture degeneration in central Australia. Part III — the assessment of grazing capacity. *Journal of the Soil Conservation Service of New South Wales* **25**: 225–250.

Condon RW, Neuman JC, Cunningham GM. 1969d. Soil erosion and pasture degeneration in central Australia. Part IV. *Journal of the Soil Conservation Service of New South Wales* **25**: 295–321.

Donovan P. 1995. In the interest of the country: a history of the Pastoral Board of South Australia 1893–1993. South Australian Department of Environment and Natural Resources.

Folland DK, Powell DP. 1994. The standard GISST data sets: version 1 and 2. Climate Research Technical Note 56, Hadley Centre, Meteorological Office, Bracknell, Berkshire, UK; 50–51.

Gershunov A, Barnett T. 1998. Inter-decadal modulation of ENSO teleconnections. *Bulletin of the American Meteorological Society* **79**: 2715–2725.

Gershunov A, Cayan DR. 2003. Heavy daily precipitation frequency over the contiguous United States: sources of climatic variability and seasonal predictability. *Journal of Climate* **16**: 2752–2765.

Gershunov A, Barnett T, Cayan D. 1999. North Pacific interdecadal oscillation seen as factor in ENSO-related North American climate anomalies. *Eos* **80**: 25–30.

Hodgkinson KC, Harrington GN, Griffin GF, Noble JC, Young MD. 1984. Management of vegetation with fire. In *Management of Australia's Rangelands*, Harrington GN, Wilson AD, Young MD (eds). CSIRO: 141–156.

Jeffrey SJ, Carter JO, Moodie KB, Beswick AR. 2001. Using spatial interpolation to construct a comprehensive archive of Australian climate data. *Environmental Modelling and Software* **16**: 309–330.

Johnston PW, McKeon GM, Day KA. 1996. Objective 'safe' grazing capacities for southwest Queensland, Australia: development of a model for individual properties. *Rangeland Journal* **18**: 224–258.

Kalnay E, Kanamitsu M, Kistler R, Collins W, Deaven D, Gandin L, Iredell M, Saha S, White G, Woollen J, Zhu Y, Chelliah M, Ebisuzaki W, Higgins W, Janowiak J, Mo KC, Ropelewski C, Wang J, Leetmaa A, Reynolds R, Jenne R, Joseph D. 1996. The NCEP/NCAR 40-year reanalysis project. *Bulletin of the American Meteorological Society* **77**: 437–471.

Landsberg RG, Ash AJ, Shepherd RK, McKeon GM. 1998. Learning from history to survive in the future: management evolution on Trafalgar Station, northeast Queensland. *Rangeland Journal* **20**: 104–118.

Madden RA, Julian PR. 1971. Detection of a 40–50 day oscillation in the zonal wind in the tropical Pacific. *Journal of the Atmospheric Sciences* **28**: 702–708.

Mann ME, Park J. 1999. Oscillatory spatio-temporal signal detection in climate studies: a multiple-taper spectral domain approach. *Advances in Geophysics* **41**: 1–131.

McKeon G, Hall W, Henry B, Stone G, Watson I. 2004. Pasture degradation and recovery in Australia's rangelands: learning from history. *Natural Resource Sciences*, Queensland Department of Natural Resources, Mines and Energy: Queensland, Australia, 256 pp.

McKeon GM, Day KA, Howden SM, Mott JJ, Orr DM, Scattini WJ, Weston EJ. 1990. Management of pastoral production in northern Australian savannas. *Journal of Biogeography* **17**: 355–372.

Noble JC. 1997. The delicate and noxious scrub: CSIRO studies on native tree and shrub proliferation in the semi-arid woodlands of eastern Australia. CSIRO, Canberra.

Parker DE, Jones PD, Folland CK, Bevan A. 1994. Interdecadal changes of surface temperature since the late nineteenth century. *Journal of Geophysical Research* **99**: 14 373–14 399.

Power S, Casey T, Folland C, Colman A, Mehta V. 1999. Interdecadal modulation of the impact of ENSO on Australia. *Climate Dynamics* **15**: 319–324.

Purvis JR. 1986. Nurture the land: my philosophies of pastoral management in central Australia. *Australian Rangeland Journal* **8**: 110–117.

Ratcliffe FN. 1937. Further observations on soil erosion and sand drift, with special reference to southwestern Queensland. Council for Scientific and Industrial Research Pamphlet No. 70.

Reynolds RW, Marsico DC. 1993. An improved real-time global sea surface temperature analysis. *Journal of Climate* **6**: 114–119.

Rogers LG, Cannon MG, Barry EV. 1997. Land resources of the Dalrymple shire. Land Use and Fisheries Project Report Series, Queensland Department of Primary Industries, Brisbane.

Simmonds I, Hope P. 1997. Persistence characteristics of Australian rainfall anomalies. *International Journal of Climatology* **17**: 597–613.

Snedecor GW, Cochran WG. 1980. *Statistical Methods*. Iowa State University Press: Ames, IA.

Stone RC, Hammer GL, Marcussen T. 1994. Prediction of global precipitation probabilities using phases of the southern oscillation index. *Nature* **354**: 252–255.

Tourre YM, Rajagopalan B, Kushnir Y, Barlow M, White WB. 2001. Patterns of coherent decadal and interdecadal climate signals in the Pacific basin during the 20th century. *Geophysical Research Letters* **28**: 2069.

Warrego Graziers Association. 1988. Submission to the United Graziers Association on the degradation of southwest Queensland. WGA, Charlesville, Queensland, Australia.

White WB, Cayan DR. 1998. Quasi-periodicity and global symmetries in interdecadal upper ocean temperature variability. *Journal of Geophysical Research* **103**: 21 335–21 354.

White WB, Tourre YM. 2003. Global SST/SLP waves during the 20th century, *Geophysical Research Letters* **30**(12): 1651. DOI: 10.1029/2003GL017055.

White WB, McKeon G, Syktus J. 2003. Australian drought: the interference of multi-spectral global standing modes and travelling waves. *International Journal of Climatology* **23**: 631–662.

Wilcox DG, Cunningham GM. 1993. Economic and ecological sustainability of current land use in Australia's range lands. In *R&D for Sustainable Use and Management of Australia's Rangelands. Proceedings of a National Workshop*. LWRRDC Occasional Paper Series No. 06/93; 87–171.